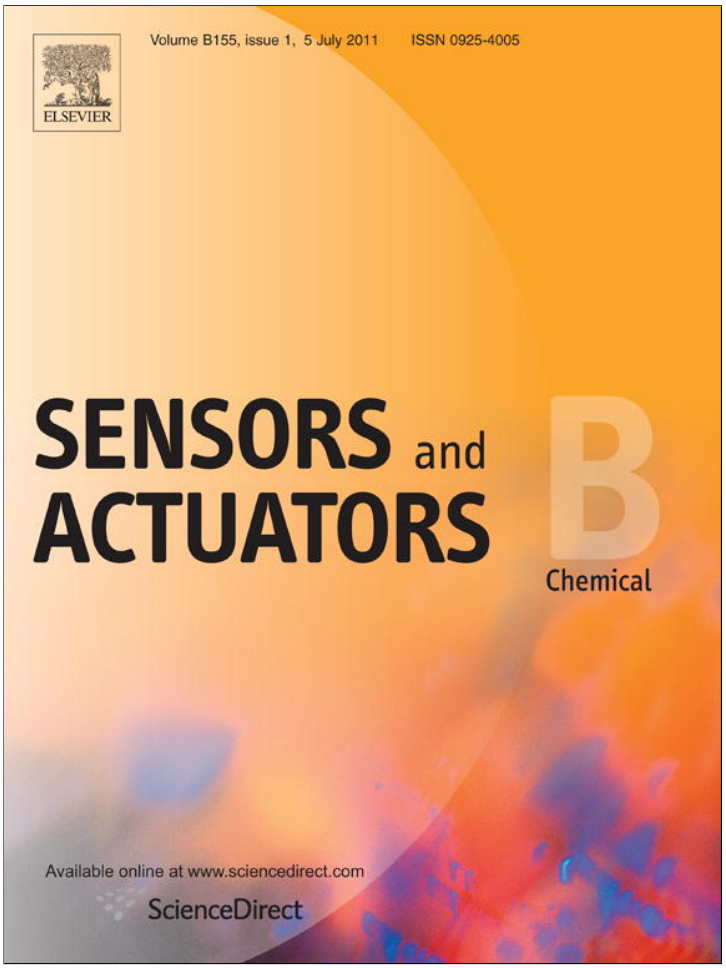

Sensors and Actuators B 155 (2011) 375–379

Contents lists available at ScienceDirect

Sensors and Actuators B: Chemical

journal homepage: www.elsevier.com/locate/snb

Short communication

Enhanced surface plasmon resonance detection of DNA hybridization based on ZnO nanorod arrays

Kyung Min Byun[a], Nak-Hyeon Kim[a], Yeong Hwan Ko[b], Jae Su Yu[b,*]

[a] Department of Biomedical Engineering, Kyung Hee University, Yongin 446-701, Republic of Korea
[b] Department of Electronics and Radio Engineering, Kyung Hee University, 1 Seocheon-dong, Giheung-gu, Yongin 446-701, Republic of Korea

ARTICLE INFO

Article history:
Received 17 September 2010
Received in revised form
18 December 2010
Accepted 20 December 2010
Available online 28 December 2010

Keywords:
Surface plasmon resonance
Biosensor
ZnO nanorod
Sensitivity enhancement
Effective medium theory

ABSTRACT

We demonstrated an enhanced surface plasmon resonance detection incorporating ZnO nanorod arrays (NRAs) built on a thin gold film. ZnO NRAs were fabricated by wet chemical growth method and used for the detection of DNA hybridization. Experimental results exhibited that ZnO NRAs provided a notable sensitivity improvement by more than 3 times, which is attributed to an increase in the surface reaction area. The measured sensitivity enhancement matched well with the numerical analyses based on the effective medium theory. Our approach is intended to show the feasibility and extend the applicability of the ZnO-based SPR biosensor to diverse biomolecular binding events.

1. Introduction

Among various optical biosensing schemes, surface plasmon resonance (SPR) is a surface-sensitive technique based on the principle to measure a refractive index change caused by biomolecular adsorption occurring at a noble metal film. By measuring the shift of resonance angle in response to the biomolecular interactions, SPR biosensors can detect various binding reactions on a quantitative basis in real time. Conventionally, the Kretschmann configuration has been used for resonant excitation of surface plasmons. The traditional thin-metal-film-based SPR biosensor has a sensitivity limit of as high as 5×10^{-7} refractive index units, which corresponds to a concentration of 1 pg/mm^2 [1].

Since an enhanced sensitivity allows the detection of target analytes of low molecular weight or in low concentration, interesting approaches for SPR signal amplification have been proposed, for example, using biomolecule-tagged colloidal gold nanoparticles [2], magneto-optic effects [3], surface relief nanostructure-mediated localized SPR (LSPR) [4,5], metal-clad waveguides [6], and phase-sensitive SPR detections [7]. Note that, due to the improved reproducibility and no requirements of external labels, the use of periodic metallic nanostructures such as nanogratings and nanoposts directly built on a metal film has been the topic of recent theoretical and experimental studies and has resulted in a significant signal enhancement [5,8]. However, since these methods require difficult and expensive fabrication processes, especially for finer nanostructures, it is greatly desired to develop a cost-effective SPR substrate with an enhanced sensing performance.

The sensitivity of the conventional SPR biosensor can be simply improved by increasing the surface reaction area because the SPR response relies on the amount of interactions between the immobilized capture ligand and the complementary target analyte at the sensor surface. In this study, we intend to prove the SPR signal enhancement induced by ZnO nanorod arrays (NRAs) with the simplicity in fabrication and the good uniformity over large surface areas. To demonstrate the effect of ZnO NRAs on the sensitivity enhancement experimentally, DNA hybridization in buffer solutions was employed as a layer with a refractive index contrast in the course of biomolecular adsorption.

2. Materials and methods

A thin gold film of 40 nm was evaporated on an SF10 glass substrate after an evaporation of 2-nm thick chromium adhesion layer. The ZnO NRAs were then fabricated by wet chemical growth method. A 3 nm-thick ZnO seed layer was deposited by RF magnetron sputter using a ZnO target (99.999% purity) at room temperature because this method allowed the accurate thickness control and the good reproducibility/stability. The samples were vertically immersed into aqueous solution with an equivalent zinc

* Corresponding author. Tel.: +82 31 201 3820.
E-mail address: jsyu@khu.ac.kr (J.S. Yu).

0925-4005/$ – see front matter © 2010 Elsevier B.V. All rights reserved.
doi:10.1016/j.snb.2010.12.039

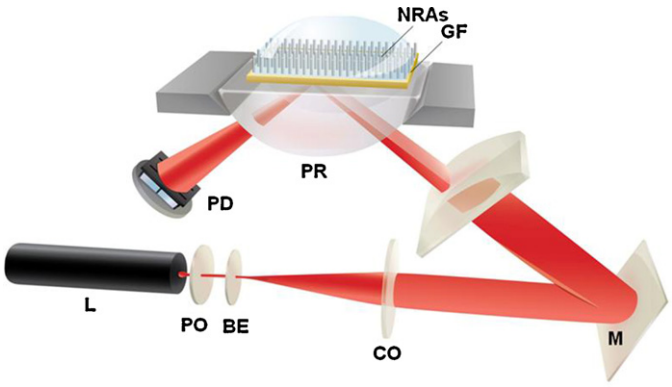

Fig. 1. Schematic diagram of the experimental setup with an intensity-based angular interrogation scheme to measure SPR signals of the ZnO NRAs-based SPR substrate. (L: laser, PO: polarizer, BE: beam expander, CO: collimator, M: mirror, PR: prism, PD: photodetector, GF: gold film, and NRAs: nanorod arrays).

nitrate hydrate and hexamethylenetetramine concentration at a temperature of 95 °C for 5 h under constant stirring. To investigate an influence of the density and geometry of ZnO NRAs on the sensitivity of the SPR biosensor, we would take into account two molar concentrations of zinc nitrate at 2 and 10 mM.

The fabricated SPR substrates based on ZnO NRAs were measured using an experimental setup with an intensity-based angular interrogation scheme (Fig. 1) and compared with the conventional SPR structure without nanorods. The optical setup consists of a polarized He–Ne laser (10 mW, $\lambda = 633$ nm, 25-LHP-991, Melles Griot, Carlsbad, CA) and dual rotation stages (URS75PP, Newport, Irvine, CA), pre-aligned for the sensor chip and a photodiode (818-UV, Newport, Irvine, CA), with a nominal resolution of 0.002°. The minimum measurable refractive index difference of our setup was estimated to be in the range of $\Delta n \sim 1 \times 10^{-6}$ [8]. It is noted that, since we are interested only in the net resonance shift before and after DNA hybridization, the setup does not detect the details of intermediate binding kinetics. Moreover, multiple sites in a given sample were measured to ensure the consistency and thereby reduce the standard deviation.

Protocols for DNA hybridization are as follows. We used HPLC-purified capture oligonucleotide and its complementary target oligonucleotide purchased from Genotech Inc. (Taejeon, Korea). The base sequences were 5′-Thiol-ATT GGA CAC GAG ACG CAA TG-3′ for capture probes and 5′-CAT TGC GTC TCG TGT CCA AT-3′ for target probes. Immobilization buffer of 1 M KH_2PO_4 and hybridization buffer of 1 M NaCl, 10 mM Tris-buffer, pH 7.4, and 1 mM EDTA were used. Dithiothreitol and ethyl acetate purchased from Sigma–Aldrich (Saint Louis, MO, USA) were used to make a covalent linkage from thiol-labeled capture probe. Contrary to our protocol, commercial SPR devices employ the dextran hydrogel surface to provide a fast and efficient covalent coupling of ligands, thereby leading to an improvement in the immobilization capacity and the sensitivity [9].

All stock oligonucleotide solutions were stored at −20 °C and made with the distilled and deionized water (DDW). To detect the DNA hybridization, the capture DNA was first immobilized on the SPR sensor substrates. After the sensor chip was soaked briefly in the DDW and the SPR response became stable, 1 μM target DNA was injected and SPR characteristics were monitored until no SPR angle change was observed. Before loading the sensor chip onto the measurement setup, the modified samples were rinsed with ethanol and DDW as rapidly as possible and dried by blowing nitrogen. In terms of the solubility of ZnO, the interaction of ZnO nanostructures with different solutions, including deionized water, ammonia, NaOH solution, and horse blood serum has been

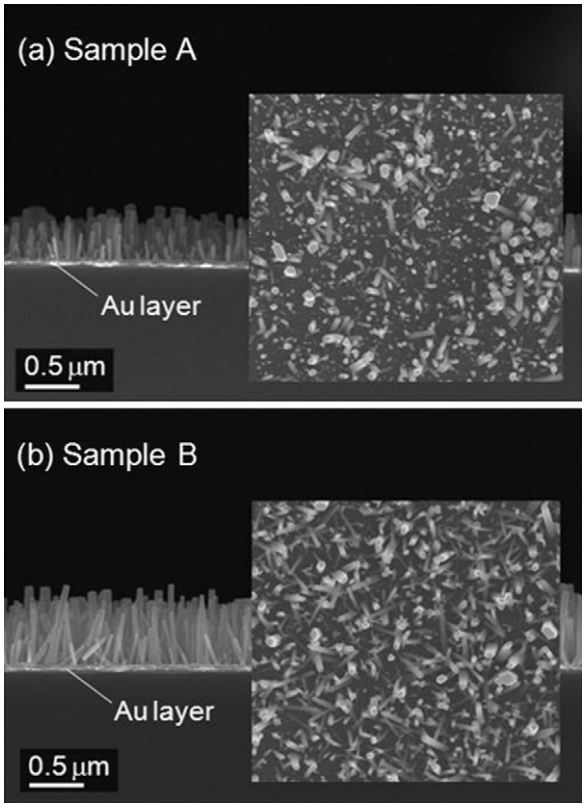

Fig. 2. Cross section and top view SEM images of ZnO NRAs grown with the sputtered ZnO seed layer on the thin gold film for zinc nitrate concentrations of (a) 2 mM and (b) 10 mM.

investigated [10]. In particular, the results showed that ZnO can be dissolved by deionized water (pH = 4.5–5.0) and the ZnO solubility decreases as its pH increases from acidic to neutral condition. In our case, we used the DDW for brief rinsing and the buffer solutions at around pH ∼ 7, so that the minimum possibility for ZnO solubility was realized.

3. Results and discussion

Fig. 2 shows the cross section and top view scanning electron microscope (SEM) images of ZnO NRAs grown with the sputtered ZnO seed layer on the gold film for zinc nitrate concentrations of (a) 2 mM and (b) 10 mM, designated as Sample A and Sample B. The ZnO NRAs were crystallized in hexagonal wurzite structures. The measured geometric parameters of ZnO NRAs are presented in Fig. 3. As the zinc nitrate concentration increased, the NRAs became denser with relatively improved vertical alignments due to the increased Zn^{2+} ions and OH^- ions. The density of nanorods in 1 μm^2 was increased from 45.4 at 2 mM to 81.4 at 10 mM. The average height of ZnO NRAs also increased largely from 302.5 nm at 2 mM to 546.6 nm at 10 mM, while the average width was kept 41.9 and 53.6 nm at 2 and 10 mM, respectively.

Fig. 4 shows the dependences of the SPR curves and sensitivity characteristics on the density and geometry of ZnO NRAs. The resonance angles before applying target DNA were obtained to be 57.79° for reference, 58.43° for Sample A, and 62.45° for Sample B, respectively. Fair increment in plasmon angle is attributed to denser and larger ZnO NRAs that may induce the local refractive index on a thin metal film to increase effectively. In Fig. 4(a), for conventional SPR substrate, the resonance angles before and after DNA hybridization were 57.79° and 57.84°; thus, the resonance shift was 0.05°. On the other hand, ZnO NRAs-based samples exhibited a pronounced res-

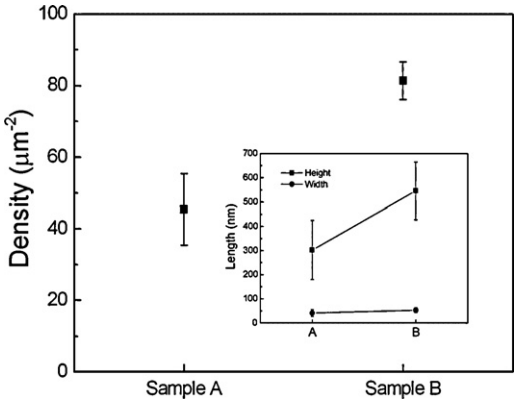

Fig. 3. The density of ZnO NRAs for two working SPR samples. The inset shows the average height and width of ZnO NRAs.

onance change with an increase of the number of nanorod arrays, as listed in Table 1. The sensitivity enhancement factor (SEF) [4], defined as the ratio $\Delta\theta_{SPR}$ (with NRAs)/$\Delta\theta_{SPR}$ (without NRAs), is determined to be 2.2 ± 0.25 for Sample A, and 3.4 ± 0.30 for Sample B, indicating a notable increase in sensitivity (Fig. 4(b)). This enhancement is mainly associated with an increased surface reaction area provided by ZnO NRAs. An increment of surface reaction area allows additional interactions between the sensor substrate and the adsorbed target analytes. Strong correlation between the surface-limited increase of binding area and the enhanced sensitivity was also reported by Oh et al., representing a prominent amplification in the resonance shift by employing mesoporous silica substrates with a high pore volume [11].

On the contrary, the limit of detection (LOD), which is another important sensing performance, was found to be degenerated for ZnO NRAs-based SPR samples. From the relation of $LOD = 3.3\sigma/S$, where σ is the standard deviation and S is the slope of the calibration curve, the LOD values became worse by 4.2 times for Sample A and 5.0 times for Sample B, compared to the conventional SPR biosensor. This adverse effect is attributable to the increased uncertainty caused by the broadening of SPR curve and the non-uniform distribution of ZnO NRAs. In other words, the broader SPR curve and the local variations in the density and height of ZnO NRAs can affect the high standard errors when determining the SPR angles, and finally lead to a notable degradation of the LOD performance. However, we may resolve the problem by realizing the uniform geometry and coverage of ZnO NRAs over large areas through a further optimization of the chemical growth process.

Table 1
Measured SPR characteristics and SEF values.

Type	SPR angle shift (°)		SEF
	Average	Standard error	
Reference	0.05	0.003	1.0
Sample A	0.11	0.028	2.2
Sample B	0.17	0.051	3.4

Next, in order to analyze the results of SEF characteristics theoretically, the well-established effective medium theory is applied. In our calculation, ZnO nanorod is modeled as a cylindrical structure with a circular cross-section. The volume fraction f_{ZnO} of ZnO nanorods and the refractive index n_{ZnO} of bulk ZnO can be used to determine the effective refractive index neff of the composite layer with ZnO NRAs. For cylindrical nanorods, the volume fraction values were equal to $f_{ZnO} = 0.063$ for Sample A and $f_{ZnO} = 0.184$ for Sample B. In the Bruggermann effective medium approximation [12,13], the following expression holds for the effective refractive index of the layer including ZnO NRAs.

$$f_{ZnO}\frac{n_{ZnO}^2 - n_{eff}^2}{n_{ZnO}^2 + 2n_{eff}^2} + (1 - f_{ZnO})\frac{n_{env}^2 - n_{eff}^2}{n_{env}^2 + 2n_{eff}^2} = 0, \quad (1)$$

where n_{env} is the refractive index of dielectric medium surrounding the sensor surface, which involves DNA hybridization event. In computation, the target analytes covering the whole substrate surface were modeled as a 3-nm thick homogeneous single-stranded DNA monolayer and its refractive index changed from 1.462 to 1.480 with the formation of the double-stranded DNA [14,15]. The optical constants (n, k) of an SF10 glass substrate, chromium, gold, and ZnO were taken as (1.723, 0), (3.48, 4.36), (0.18, 3.00), and (1.989, 0) at $\lambda = 633$ nm [16]. After determining n_{eff} values for individual effective media before and after hybridization, we used the transfer-matrix method (TMM) to obtain the reflectance characteristics of the SPR samples. The TMM has been extensively used and well-validated for calculation of the multilayered optical system. For details on our TMM routine, readers are advised to refer to Ref. [17]. We performed the TMM computation by scanning the incidence angle of a TM-polarized plane wave with an angular resolution of 0.01°.

The numerical results in Fig. 5, obtained by Eq. (1) and the TMM, imply the strong dependence of the SEF value on the nanorod height, when we assume that the density and width of nanorods are

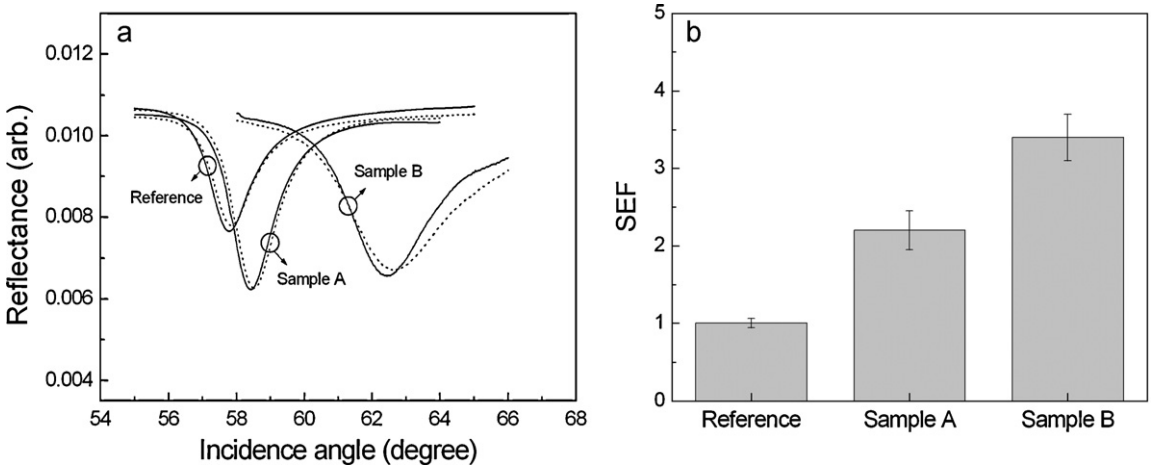

Fig. 4. (a) SPR responses and (b) Statistical data of SEF value of the three working samples for DNA hybridization experiments. The solid and dotted lines represent the SPR curves before and after DNA hybridization, respectively.

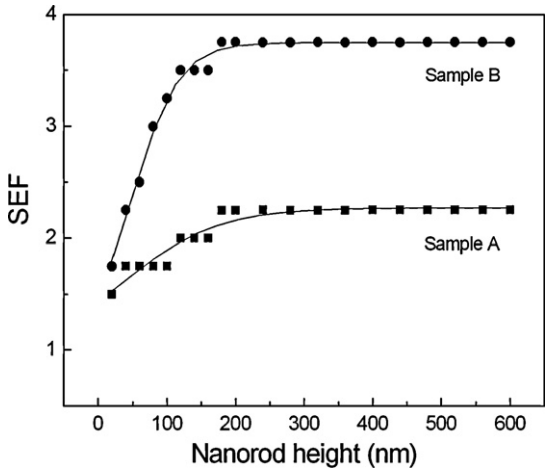

Fig. 5. Calculated SEF as a function of nanorod height, assuming that the density and width of ZnO NRAs are equal to the values of Sample A (square) and B (circle). The solid lines indicate sigmoidal fits of numerical data.

equal to the geometric parameters of Samples A and B. At an initial stage, the SEF value displays a rapid increment because the change in nanorod height causes the gross surface area to be effectively increased. The nanorods equivalent to the Sample B achieve a maximum SEF of 3.75, while the highest SEF obtained is 2.25 for the ZnO nanorods whose density and width correspond to the Sample A. As a result, the measured SEFs in Table 1 are in good agreement with numerical data in Fig. 5, indicating that the Bruggermann approximation works well for this composite material system. In particular, the contrast in SEF seems evident due to the fact that the greater number of nanorods can provide more rooms for target analytes attached to the sensor substrates.

Finally, it is interesting to find in Fig. 5 that, when the nanorod height is larger than 200 nm, the SEF reaches a maximum and saturates in both cases. No further increase of SEF can be explained by the limited penetration depth of plasmon waves with rapidly decaying intensity when one moves away from the metal surface. Since the detection range of the SPR biosensor is intrinsically confined to the penetration depth with a dimension of several hundred nanometers [18], an increase of nanorod height over the plasmon decay length may not contribute to the additional sensitivity enhancement. Based on this plasmonic interpretation, we can analyze the correlation between the surface reaction area and the sensitivity improvement quantitatively. Assuming that the surface area beyond the penetration depth of about 200 nm has no effect on the enhancement of sensitivity, the effective surface area growth factor (SAGF), the ratio of the effective surface reaction area of cylindrical ZnO NRA-based SPR substrates to that of the conventional SPR substrate, was calculated using the geometric parameters shown in Fig. 3. The results presented that SAGF = 2.13 for Sample A and SAGF = 3.56 for Sample B and these SAGF values are consistent with the SEF characteristics in Table 1. It is, therefore, apparent that the surface reaction area plays an important role in characterizing the sensitivity performance of the proposed SPR substrates with ZnO NRAs. As subsequent works, to achieve an additional sensitivity gain, the development of the sensor substrate with an enlarged penetration depth [19] and the use of metallic nanoparticles combined with the ZnO-based SPR substrates are currently under investigation.

4. Conclusions

This study presented the ZnO NRAs-enhanced SPR detection of DNA hybridization. From the results presenting notably amplified optical responses by more than 3 times, a promising potential of ZnO NRAs for enhanced detection of target analytes was demonstrated experimentally. Due to the simplicity in fabrication process and the uniform coverage over large areas, it is expected that ZnO NRAs could be used to augment the surface binding area enormously for a variety of chemical and biological biosensors.

Acknowledgements

Kyung Min Byun and Jae Su Yu acknowledge the support of Korea Science and Engineering Foundation (KOSEF) grant funded by the Korean government (MEST) (2010-0005137 and 2009-0070459, respectively).

Appendix A. Supplementary data

Supplementary data associated with this article can be found, in the online version, at doi:10.1016/j.snb.2010.12.039.

References

[1] J. Homola, S.S. Yee, G. Gauglitz, Surface plasmon resonance sensors: review, Sens. Actuators B 54 (1999) 3–15.
[2] L. He, M.D. Musick, S.R. Nicewarner, F.G. Salinas, S.J. Benkovic, M.J. Natan, C.D. Keating, Colloidal Au-enhanced surface plasmon resonance for ultrasensitive detection of DNA hybridization, J. Am. Chem. Soc. 122 (2000) 9071–9077.
[3] B. Sepúlveda, A. Calle, L.M. Lechuga, G. Armelles, Highly sensitive detection of biomolecules with the magneto-optic surface-plasmon-resonance sensor, Opt. Lett. 31 (2006) 1085–1087.
[4] K.M. Byun, S.J. Yoon, D. Kim, S.J. Kim, Experimental study of sensitivity enhancement in surface plasmon resonance biosensors by use of periodic metallic nanowires, Opt. Lett. 32 (2007) 1902–1904.
[5] L. Malic, B. Cui, T. Veres, M. Tabrizian, Enhanced surface plasmon resonance imaging detection of DNA hybridization on periodic gold nanoposts, Opt. Lett. 32 (2007) 3092–3094.
[6] N. Skivesen, R. Horvath, H.C. Pedersen, Optimization of metal-clad waveguide sensors, Sens. Actuators B 106 (2005) 668–676.
[7] P.P. Markowicz, W.C. Law, A. Baev, P.N. Prasad, S. Patskovsky, A. Kabashin, Phase-sensitive time-modulated surface plasmon resonance polarimetry for wide dynamic range biosensing, Opt. Express. 15 (2007) 1745–1754.
[8] K. Kim, D.J. Kim, S. Moon, D. Kim, K.M. Byun, Localized surface plasmon resonance detection of layered biointeractions on metallic subwavelength nanogratings, Nanotechnology 20 (2009) 315501.
[9] S. Löfås, B. Johnsson, A novel hydrogel matrix on gold surfaces in surface plasmon resonance sensors for fast and efficient covalent immobilization of ligands, J. Chem. Soc. Chem. Commun. 21 (1990) 1526–1528.
[10] J. Zhou, N. Xu, Z.L. Wang, Dissolving behavior and stability of ZnO wires in biofluids: a study on biodegradability and biocompatibility of ZnO nanostructures, Adv. Mater. 18 (2006) 2432–2435.
[11] S. Oh, J. Moon, T. Kang, S. Hong, J. Yi, Enhancement of surface plasmon resonance signals using organic functionalized mesoporous silica on a gold film, Sens. Actuators B 114 (2006) 1096–1099.
[12] D.E. Aspnes, Optical properties of thin-films, Thin Solid Films 89 (1982) 249–262.
[13] H.Y. Chen, H.W. Lin, C.Y. Wu, W.C. Chen, J.S. Chen, S. Gwo, Gallium nitride nanorod arrays as low-refractive-index transparent media in the entire visible spectral region, Opt. Express. 16 (2008) 8106–8116.
[14] D.E. Gray, S.C. Case-Green, T.S. Fell, P.J. Dobson, E.M. Southern, Ellipsometric and interferometric characterization of DNA probes immobilized on a combinatorial array, Langmuir 13 (1997) 2833–2842.
[15] S. Elhadj, G. Singh, R.F. Saraf, Optical properties of an immobilized DNA monolayer from 255 to 700 nm, Langmuir 20 (2004) 5539–5543.
[16] E.D. Palik, Handbook of Optical Constants of Solids, Academic, San Diego, 1985.
[17] S.H. Choi, K.M. Byun, Investigation on an application of silver substrates for sensitive surface plasmon resonance imaging detection, J. Opt. Soc. Am. A 27 (2010) 2229–2236.
[18] N. Skivesen, R. Horvath, S. Thinggaard, N.B. Larsen, H.C. Pedersen, Deep-probe metal-clad waveguide biosensors, Biosens. Bioelectron. 22 (2007) 1282–1288.
[19] S.J. Yoon, D. Kim, Thin-film-based field penetration engineering for surface plasmon resonance biosensing, J. Opt. Soc. Am. A 24 (2007) 2543–2549.

Biographies

K.M. Byun received the B.S. and M.S. degrees from the school of electrical engineering, Seoul National University, Seoul, Korea, and the PhD degree from Seoul National University, in 2007. From July 2007 to February 2008, he worked as a visiting scientist in the department of biomedical engineering, Cornell University, Ithaca, NY. He is currently assistant professor at the department of biomedical engineering,

Kyung Hee University, Yongin, Korea. His main research activities are theoretical and experimental studies on highly sensitive localized SPR biosensors with metallic nanostructures and microarray-based SPR imaging systems.

N.H. Kim received the B.S. degree from Konkuk University, Chungju, Korea, in 2009. He is currently working toward the M.S. degree in the department of biomedical engineering, Kyung Hee University. His primary research interest is in the area of surface-enhanced surface plasmon resonance biosensors based on metallic nanostructures.

Y.W. Ko received the B.S. and M.S. degrees from the Department of Electronics, Kyung Hee University, Korea, in 2007 and 2009, respectively. He is currently working toward the PhD degree in the Department of Electronics, Kyung Hee University. His research interest is in the area of nanostructure-based optoelectronic devices.

J.S. Yu received the B.S. degree in electronic engineering from the Kyungpook National University, Korea, in 1995, and the M.S. and PhD degrees in optoelectronic engineering from Gwangju Institute of Science and Technology (GIST), Gwangju, Korea, in 1997 and 2002, respectively. In 2002, he became a research professor in the Ultrafast Fiber-Optic Networks Research Center, GIST, Korea. He joined the Center for Quantum Devices, Northwestern University, Evanston, IL, as a Postdoctorial Fellow in Oct. 2002, where he worked on the fabrication, packaging, and characterization of optoelectronic devices. Since joining in Sept. 2006, he is currently an associate professor in the Department of Electronics and Radio Engineering and Director of the Institute for Laser Engineering, Kyung Hee University, Korea. His research interests include solar cells, light emitting diodes, optical sensors, nanostructures, and nanophotonics.